# Techniques for heavy-ion coupled-channels calculations. I. Long-range Coulomb coupling

M. Rhoades-Brown, M. H. Macfarlane, and Steven C. Pieper
*Argonne National Laboratory, Argonne, Illinois 60439*
(Received 6 September 1979)

Direct-reaction calculations for heavy ions require special computational techniques that take advantage of the physical peculiarities of heavy-ion systems. This paper is the first of a series on quantum-mechanical coupled-channels calculations for heavy ions. It deals with the problems posed by the long range of the Coulomb coupling interaction. Our approach is to use the Alder-Pauli factorization whereby the channel wave functions are expressed as products of Coulomb functions and modulating amplitudes. The equations for the modulating amplitudes are used to integrate inwards from infinity to a nuclear matching radius ($\approx 20$ fm). To adequate accuracy, the equations for the amplitudes can be reduced to first order and solved in first Born approximation. The use of the Born approximation leads to rapid recursion relations for the solutions of the Alder-Pauli equations and hence to a great reduction in computational labor. The resulting coupled-channels Coulomb functions can then be matched in the usual way to solutions of the coupled radial equations in the interior region of $r$ space. Numerical studies demonstrate the reliability of the various techniques introduced.

[NUCLEAR REACTIONS HI coupled-channel inelastic scattering. Treatment of long-range Coulomb potential.]

## I. INTRODUCTION

Models of nuclear direct reactions are based on the identification of a few privileged reaction channels, usually the elastic channel and those particularly strongly coupled to it. The Schrödinger equation is then solved in the model space spanned by these privileged channels. The influence of channels excluded from the model space is either taken into account statistically or expressed by absorptive components in the effective interaction potentials that act within the truncated model space. In a partial-wave configuration-space representation, reaction models of the sort under consideration lead to sets of coupled integro-differential equations for radial wave functions. The number of coupled equations ($N$) for a given total angular momentum and parity ($J, \pi$) is usually several times as large as the number of channels in the model space because there are usually several distinct ways to couple the internal nuclear spins and the orbital angular momentum of the relative motion to a given total angular momentum.

The numerical complexity of coupled-channels calculations has severely inhibited the study of nuclear direct reactions. The standard procedure is to solve the $N$ coupled radial equations $N$ times with linearly independent regular starting values. The equations are integrated from the origin to a joining radius $R_\infty$ at which all nuclear and coupling interactions have become insignificant. A single linear combination with the appropriate asymptotic behavior (incoming and outgoing waves in the elastic channel, outgoing waves in all others) is then constructed; in the process the desired $S$-matrix elements are found. This method is satisfactory for light-ion reactions but is particularly inefficient for heavy-ion reactions. The long range of the Coulomb coupling interaction, the small step size necessitated by the short wavelength, and the large number of partial waves that contribute significantly have restricted fully quantum-mechanical coupled-channels calculations for heavy ions to at most three or four reaction channels—clearly inadequate to address the key physical questions in the field.

Many-channel calculations have been possible only within the semiclassical framework pioneered by Alder and Winther[1] for multiple Coulomb excitation. This approach has a number of limitations. Its accuracy decreases steadily as the excitation energy of the reaction channels increases. Its accuracy for particle-transfer reactions is largely untested. At energies significantly above the Coulomb barrier the computational complexity of accurate semiclassical calculations increases rapidly; alternatively, the accuracy of the simplest sort of semiclassical calculation rapidly decreases. Thus, although semiclassical methods are indispensable within their natural bailiwick, their limitations are such that a fully quantum-mechanical alternative that can cope with more than three or four reaction channels is worth seeking.

This paper is the first of a series that will describe numerical methods for quantum-mechanical coupled-channels calculations for heavy ions.

The methods to be presented in this series differ from those conventionally used in light-ion studies in three significant respects.

(1) Exploitation of the semiclassical aspects of Coulomb excitation. In light-ion coupled-channels calculations, the solutions of the coupled equations in the interior region (the region wherein nuclear and coupling potentials are significant) are joined to Coulomb functions at a joining radius $R_\infty$ (~20 fm for light ions) characteristic of the outer limit of nuclear and coupling interactions. In heavy-ion reactions the effects of Coulomb excitation are often large and produce significant channel-coupling effects out to distances of hundreds or even thousands of fm. Extension of the boundary of the interior region to the outer limit of Coulomb excitation is catastrophically inefficient. If the coupled equations for Coulomb excitation are integrated inwards from infinity to the nuclear joining radius $R_N$, the channel wave functions are found to be Coulomb functions modulated by factors that vary slowly with $r$. As first shown by Alder and Pauli,[2] the coupled equations for the modulating amplitudes can be integrated to adequate accuracy more rapidly by an order of magnitude than the original equations. The resulting coupled-channels Coulomb functions are then matched to the interior solutions at the nuclear joining radius $R_N$. The time taken to calculate the effects of Coulomb excitation is then at worst comparable to the time needed to generate the internal solutions.

(2) Iterative solutions of the coupled equations within the range of nuclear interactions. The wasteful conventional strategy, whereby the coupled equations are solved $N$ times to produce the one desired solution, can be avoided either by expansion of the channel wave function in terms of a fixed basis[3] or by iterative techniques.[4] We find that the sequential-iteration method of Raynal,[4] with Padé approximants to accelerate convergence of the $S$-matrix elements, is ideally suited to our present purposes. In all cases considered, it yields $S$-matrix elements accurate to 1 or 2% in about four iterations. (This number is the average over all contributing partial waves. Five or six iterations may be needed in grazing partial waves, only two or three in others.)

(3) Extensive use of partial-wave interpolation and extrapolation. Huge numbers of partial waves typically contribute significantly to heavy-ion cross sections. On the other hand, the underlying semiclassical features of heavy-ion interactions result in $S$ matrices that are smooth functions of the total angular momentum. It is therefore possible to calculate $S$-matrix elements directly at rather widely spaced angular momenta and to supplement these calculated matrix elements by interpolation and extrapolation. For example, in computing cross sections for the elastic scattering of 800 MeV $^{132}$Xe ions on $^{208}$Pb and for the inelastic excitation of the first $2^+$ excited state of Xe, 2000 partial waves contribute significantly, but only 25 need be treated explicitly to produce cross sections accurate to 1 or 2%. The necessary interpolation techniques have already been used[5] extensively in distorted-wave Born approximation (DWBA) studies of heavy-ion induced inelastic scattering and transfer reactions.

We believe that these techniques—the Alder-Pauli method for multiple Coulomb excitation, iterative solution of coupled equations in the interior region, and partial-wave interpolation and extrapolation—will combine to accelerate heavy-ion coupled-channels calculations by factors of 10 to 100 over the previous state-of-the-art. In this paper we are concerned with the first of the above aspects, the semiclassical nature of Coulomb excitation. The other two aspects of heavy-ion coupled-channels equations will be discussed in subsequent papers.

In Sec. II the notation to be used in this series is described, and the structure of the coupled equations for the radial functions is discussed. Section III presents the Alder-Pauli factorization of the radial wave functions for multiple Coulomb excitation; coupled equations are derived for the slowly-varying factors that modulate the asymptotic Coulomb functions. We show that under certain commonly satisfied conditions it is possible to solve these equations in first Born approximation, using integrals similar to those encountered in the DWBA for inelastic scattering. Section IV presents numerical studies of the methods developed in Sec. III, and Sec. V contains our conclusions.

## II. COUPLED EQUATIONS FOR INELASTIC SCATTERING

We consider inelastic collisions between nuclei $a$ and $A$ and ignore all processes that can occur other than elastic scattering or inelastic excitation. Let $\vec{r}$ be the relative position vector of the centers of mass of projectile $a$ and target $A$ and let $x_a$ and $x_A$ be internal nuclear coordinates. We assume that the Hamiltonian of the system has the form

$$H = H_a(x_a) + H_A(x_A) + T + V(\vec{r}, x_a, x_A), \tag{2.1}$$

where $H_a, H_A$ are the internal Hamiltonians of projectile and target and $T$ is the relative kinetic energy operator. The interaction potential $V$ contains the nuclear and Coulomb components

$V_N(r)$, $V_c(r)$ of the optical potential and the nuclear and Coulomb transition potentials $V_N(\vec{r},x_a,x_A)$, $V_c(\vec{r},x_a,x_A)$ that couple internal excitations of $a,A$ with the relative motion:

$$V(\vec{r},x_a,x_A)=V_N(r)+V_c(r)+V_N(\vec{r},x_a,x_A)+V_c(\vec{r},x_a,x_A)\,. \tag{2.2}$$

Next we construct a complete set of channel eigenstates of definite angular momentum $J$ and parity $\pi$. The internal states of $a$ and $A$ are eigenstates of the internal Hamiltonians $H_a$ and $H_A$:

$$(H_a-\mathcal{E}_a^{J_a})\Phi_{M_a}^{aJ_a}(x_a)=0\,,$$
$$(H_A-\mathcal{E}_A^{J_A})\Phi_{M_A}^{AJ_A}(x_A)=0\,, \tag{2.3}$$

where $a,A$ distinguish different internal states of given angular momentum and the energies are excitation energies referred to the respective ground states.

The space corresponding to a pair $(aJ_a,AJ_A)$ of internal states of projectile and target will be referred to as a "channel." The states in this channel have a $(2J_a+1)(2J_A+1)$-fold spin degeneracy; we introduce eigenstates

$$\Phi^{aJ_a,AJ_A,S}(x_a,x_A)=[\Phi^{aJ_a}(x_a)\times\Phi^{AJ_A}(x_A)]_M^S\,, \tag{2.4}$$

of the channel spin $\vec{S}=\vec{J}_a+\vec{J}_A$, where we have ignored the effects of antisymmetry between projectile and target nucleons. A basis state $\alpha$ for given $J,\pi$ is specified by a definite channel, a definite channel spin, and a definite relative orbital angular momentum $l_\alpha$. Solutions of the Schrödinger equation can then be expressed in terms of the basis states $\alpha$ in the form

$$\Psi_M^{J\pi}(\vec{r},x_a,x_A)=\frac{1}{r}\sum_\alpha R_\alpha^{J\pi}(r)\psi_{\alpha M}^{J\pi}(\hat{r},x_a,x_A)\,, \tag{2.5}$$

where

$$\psi_{\alpha M}^{J\pi}(\hat{r},x_a,x_A)=[i^{l\alpha}Y^{l\alpha}(\hat{r})\times\Phi^{aJ_a,AJ_A,S\alpha}(x_a,x_A)]_M^J\,.$$

In practice, only a few channels can be included in the expansion (2.5). Within the truncated model space so defined, the Schrödinger equation for each value of $J,\pi$ reduces to a finite set of coupled radial equations[6]:

$$\left(\frac{d^2}{dr^2}-\frac{l_\alpha(l_\alpha+1)}{r^2}-U_\alpha^{\rm opt}+k_\alpha{}^2\right)R_\alpha^{J\pi}(r)=\sum_{\beta=1}^{N}U_{\alpha\beta}R_\beta^{J\pi}(r)\,, \tag{2.6}$$

where the coupling matrix is

$$U_{\alpha\beta}(r)=\frac{2\mu_\alpha}{\hbar^2}\int d\hat{r}\,dx_a\,dx_A\psi_\alpha^{J\pi}(\hat{r},x_a,x_A)\times[V_N(\vec{r},x_a,x_A)+V_c(\vec{r},x_a,x_A)]\times\psi_\beta^{J\pi}(\hat{r},x_a,x_A)\,, \tag{2.7}$$

and $U_\alpha^{\rm opt}$ is $2\mu_\alpha/\hbar^2$ times the optical potential. Here $N$ is the number of coupled equations for angular momentum $(J,\pi)$, and the channel wave number $k_\alpha$ is given by

$$k_\alpha{}^2=\frac{2\mu_\alpha}{\hbar^2}(E-\mathcal{E}_A^{J_A}-\mathcal{E}_a^{J_a})\,. \tag{2.8}$$

In these formulas, $E$ is the center-of-mass energy in the incident channel, and $\mu_\alpha$ is the reduced mass in channel $\alpha$.

Solutions of the set (2.6) of coupled differential equations are required that are regular at the origin $[R_\alpha(0)=0]$ and have the asymptotic form

$$R_\alpha^{J\pi}(r)\underset{r\to\infty}{=}\frac{i}{2}\left[I_{\alpha_0}(r)\delta_{\alpha\alpha_0}-\left(\frac{k_{\alpha_0}}{k_\alpha}\right)^{1/2}S_{\alpha\alpha_0}^{J\pi}O_\alpha(r)\right], \tag{2.9}$$

where $\alpha_0$ is the incident channel and $I_\alpha,O_\alpha$ are incoming and outgoing Coulomb functions. If the channel spin for the incident channel is nonzero, there will be several basis states $\alpha_0$ with incoming components; we ignore this minor complication here. There are $N$ linearly independent regular solutions of Eqs. (2.6); the asymptotic condition (2.9) uniquely defines the desired element of the $N$-dimensional vector space that they span, including normalization. Conventional techniques for the solution of the coupled equations involve explicit construction of a complete set of $N$ regular solutions, each with a linearly independent choice of starting conditions ($dR_\alpha/dr$ at $r=0$). The coefficients of the linear combination of these solutions that has the asymptotic form (2.9) are determined, together with the $N$ $S$-matrix elements $S_{\alpha\alpha_0}$, by matching at a radius $r=R_\infty$ sufficiently large that all the potentials except $V_c(r)$ in Eq. (2.2) are negligible. The main point of iterative solutions of Eqs. (2.6) is to eliminate the need to solve the coupled equations $N$ times in order to construct a complete set of regular solutions.

Complete specification of the coupling matrix $U_{\alpha\beta}(r)$ requires the introduction of a detailed model for the internal nuclear states involved and specific assumptions about the nuclear interaction potential $V_N$. No general discussion of this complex task will be attempted here. We are concerned with techniques for the solution of the coupled equations (2.6). To test and compare various methods, we consider collisions between nuclei with $0^+$ ground states and allow one of the nuclei to be excited to a single state of natural parity. We believe that the conclusions drawn from these two-channel test cases have a wide range of validity.

The nuclear part of the optical potentials will

be taken to be of complex Woods-Saxon form, with the Coulomb part given by the interaction potential of a point charge with a uniform spherical charge distribution. The couplings $U_{\alpha\beta}(r)$ are calculated from the deformed optical model, with rotational eigenstates for the nuclear wave functions and the transition potential $V(\vec{r}, x_a, x_A)$ carried to first order in the deformation. Because the unexcited nucleus has spin 0, the quantity $S$ defined in Eq. (2.4) has the value $J_A$ for target excitation or $J_a$ for projectile excitation, and the coupling potential $U_{\alpha\beta}(r)$ can be expressed as a sum over multipoles $\lambda$ in the form

$$U^J_{S_\alpha l_\alpha, S_\beta l_\beta}(r) = \frac{2\mu_\alpha}{\hbar^2} \sum_\lambda A_\lambda(S_\alpha l_\alpha, S_\beta l_\beta, J) H_\lambda(r) ,$$

$$A_\lambda(S_\alpha l_\alpha, S_\beta l_\beta, J) = i^{l_\beta - l_\alpha}(-1)^{J+\lambda} \frac{\hat{S}_\alpha \hat{S}_\beta \hat{l}_\alpha \hat{l}_\beta \hat{\lambda}}{(4\pi)^{1/2}} \begin{pmatrix} S_\beta & \lambda & S_\alpha \\ 0 & 0 & 0 \end{pmatrix} \times \begin{pmatrix} l_\alpha & \lambda & l_\beta \\ 0 & 0 & 0 \end{pmatrix} \begin{Bmatrix} S_\alpha & l_\alpha & J \\ l_\beta & S_\beta & \lambda \end{Bmatrix} , \tag{2.10}$$

$$H_\lambda(r) = -(\beta^N_\lambda R_v) \frac{dV_N(r)}{dr} + \frac{3Z_A Z_a e^2}{(2\lambda+1)} (\beta^c_\lambda R^\lambda_c) \phi_c(r) ,$$

$$\phi_c(r) = \begin{cases} \dfrac{1}{r^{\lambda+1}}, & r \geq R'_c \\ \dfrac{r^\lambda}{(R'_c)^{2\lambda+1}}, & r < R'_c . \end{cases}$$

Here the symbol $\hat{a}$ stands for $\sqrt{2a+1}$; $\beta^N_\lambda$, $R_v$, $\beta^c_\lambda$, and $R_c$ are the deformation parameters and radii (nuclear and Coulomb) of the excited nucleus, and $R'_c$ is the Coulomb radius of the optical potential (the sum of the projectile and target Coulomb radii).

## III. TREATMENT OF COULOMB EXCITATION

Two distinct radii that play an important part in all subsequent discussions have been introduced. The first is the outer limit $R_N$ of all nuclear interactions. The second is the asymptotic radius $R_\infty$ beyond which only point-Coulomb interactions survive. Three regions are then to be distinguished:

(i) The interior region $0 < r < R_N$, to which nuclear interactions are restricted,

(ii) the intermediate region $R_N < r < R_\infty$, in which only the Coulomb components of optical-model and coupling potentials survive,

(iii) the true asymptotic region $r > R_\infty$, in which the wave function in each channel reduces to a combination [Eq. (2.9)] of pure Coulomb functions. We will find that in actual calculations it is possible to let $R_\infty \to \infty$ so that region (iii) is eliminated.

For $r > R_N$, the coupled equations (2.6) reduce to the equations that describe multiple Coulomb excitation[1]:

$$\left( \frac{d^2}{dr^2} - \frac{2\eta_\alpha k_\alpha}{r} - \frac{l_\alpha(l_\alpha+1)}{r^2} + k_\alpha{}^2 \right) R^{J\pi}_\alpha(r) = \sum_\beta U^c_{\alpha\beta}(r) R^{J\pi}_\beta(r) , \tag{3.1}$$

where $\eta_\alpha$ is the usual Sommerfeld parameter, and from Eqs. (2.10) the Coulomb coupling potential $U^c_{\alpha\beta}$ is given by

$$U^c_{l_\alpha S_\alpha, l_\beta S_\beta}(r) = \frac{2\mu_\alpha}{\hbar^2} \sum_\lambda A_\lambda(S_\alpha l_\alpha, S_\beta l_\beta, J) \frac{3Z_A Z_a e^2}{(2\lambda+1)} \frac{R^\lambda_c \beta^c_\lambda}{r^{\lambda+1}} . \tag{3.2}$$

In writing Eq. (3.2) we have assumed that $R_N$ has been chosen such that $R_N > R'_c$.

Solutions of Eqs. (3.1) in the region $[R_N, \infty]$ are Coulomb functions modulated by slowly varying amplitudes that reflect the influence of the coupling potentials (3.2). Following Alder and Pauli[2] and Alder, Roesel, and Morf,[7] we solve directly for the modulating amplitudes—a much easier procedure than direct integration of the original radial equations (3.1). Our procedure, in fact, is to extend the Coulomb functions $O_\alpha, I_\alpha$ for each basis state inwards from $\infty$ to $R_N$; the resulting outgoing and incoming solutions of the coupled Coulomb-excitation equations (3.1) are then matched at $r = R_N$ to iterative solutions of the original equations (2.6) in the interior region. The gain in efficiency over straightforward integration of the coupled equations (2.6) from 0 to $R_\infty$ is enormous.

### A. Introduction of modulating functions

In the intermediate region $R_N < r < \infty$, the coupled equations (3.1) have $N$ independent outgoing and $N$ incoming solutions. We define $\vec{O}_s(r)$ (a vector whose $N$ components are labeled by basis states $\alpha$) to be that outgoing solution obtained by starting at $r = \infty$ with an outgoing wave $O_s(k_s r)$ in basis state $s$, zero in all other channels, and integrating inwards to $R_N$. The incoming solution $\vec{I}_s(r)$ is defined in similar fashion. Clearly, $\vec{O}_s(r)$ $(s = 1, 2, \ldots, N)$ is a complete set of outgoing solutions and $\vec{I}_s(r)$ $(s = 1, 2, \ldots, N)$ a complete set of incoming solutions of Eqs. (3.1).

The Alder-Pauli[2] representation of the solutions $\vec{O}_s, \vec{I}_s$ is

$$\mathcal{O}_{s,\alpha}(r) = \frac{1}{\sqrt{k_\alpha}} \cdot a^{+}_{s,\alpha}(r) O_\alpha(k_\alpha r),$$
$$\mathcal{I}_{s,\alpha}(r) = \frac{1}{\sqrt{k_\alpha}} \cdot a^{-}_{s,\alpha}(r) I_\alpha(k_\alpha r), \tag{3.3}$$

where $O_\alpha, I_\alpha$ are uncoupled Coulomb functions and $\mathcal{O}_{s,\alpha}$ designates the $\alpha$th component of $\vec{\mathcal{O}}_s$. The modulating functions $\vec{a}^{\pm}_s$ (which are also $N$-component vectors) have the asymptotic behavior

$$a_{s,\alpha}(r) \underset{r\to\infty}{=} \sqrt{k_\alpha} \cdot \delta_{\alpha s},$$
$$\frac{d}{dr}\vec{a}_s(r) \underset{r\to\infty}{=} 0. \tag{3.4}$$

In terms of the coupled-channels Coulomb wave functions just introduced, the asymptotic form (2.9) of the radial wave functions is

$$R^{J\pi}_{\alpha}(r) \underset{r\to\infty}{=} \frac{i}{2}\left[\mathcal{I}_{\alpha_0,\alpha}(r) - \sum_\beta \left(\frac{k_{\alpha_0}}{k_\beta}\right)^{1/2} S^{J\pi}_{\beta\alpha_0} \mathcal{O}_{\beta,\alpha}(r)\right]. \tag{3.5}$$

The advantage of Eq. (3.5) is that it becomes valid at $r = R_N$ instead of the much larger radius $R_\infty$ at which Eq. (2.9) becomes valid.

The uncoupled Coulomb functions $I_\alpha$ and $O_\alpha$ are solutions of the homogeneous part of Eqs. (3.1). Substitution of Eqs. (3.3) in Eqs. (3.1) then yields a set of coupled second-order equations for the outgoing amplitudes:

$$\frac{d^2}{dr^2}a^{+}_{s,\alpha} + \frac{2}{O_\alpha}\frac{d}{dr}O_\alpha \frac{d}{dr}a^{+}_{s,\alpha} = \sum_\beta \left(\frac{k_\alpha}{k_\beta}\right)^{1/2} \cdot U^{c}_{\alpha\beta}(r)\frac{O_\beta}{O_\alpha} a^{+}_{s,\beta}. \tag{3.6}$$

It is also seen that the incoming solution $\vec{\mathcal{I}}_s(r)$ is the complex conjugate of the outgoing solution $\vec{\mathcal{O}}_s(r)$,

$$\vec{\mathcal{I}}_s(r) = \vec{\mathcal{O}}^{*}_s(r), \tag{3.7}$$

so that only the equations for the outgoing solutions need be considered explicitly.

### B. Approximations for the modulating functions

By a sequence of approximations, Eqs. (3.6) can be considerably simplified. To state the approximations involved, we use the phase-amplitude representation,[8]

$$\begin{pmatrix} O_\alpha \\ I_\alpha \end{pmatrix} = \frac{e^{\pm i\phi_\alpha}}{\sqrt{\zeta_\alpha}}, \tag{3.8}$$

of the Coulomb functions. The asymptotic phase is given by

$$\phi_\alpha \underset{r\to\infty}{=} k_\alpha r - \eta_\alpha \ln 2k_\alpha r + \sigma_\alpha - \frac{l_\alpha \pi}{2}, \tag{3.9}$$

where $\sigma_\alpha$ is the Coulomb phase shift. Outside the Coulomb turning point, $\zeta_\alpha$ is a very slowly varying function of $r$ that increases monotonically towards its asymptotic value of unity

$$\zeta_\alpha \underset{r\to\infty}{=} 1. \tag{3.10}$$

The Wronskian relation for Coulomb functions reduces to

$$\frac{d}{dr}\phi_\alpha = k_\alpha \zeta_\alpha. \tag{3.11}$$

In this representation, the coefficients in the coupled equations (3.6) become

$$\frac{1}{O_\alpha}\frac{dO_\alpha}{dr} = k_\alpha\left(i\zeta_\alpha - \frac{1}{2k_\alpha}\frac{d}{dr}\zeta_\alpha\right), \tag{3.12}$$

$$\frac{O_\beta}{O_\alpha} = \left(\frac{\zeta_\alpha}{\zeta_\beta}\right)^{1/2} e^{i(\phi_\beta - \phi_\alpha)}. \tag{3.13}$$

Two approximations can now be made to exploit the fact that the various amplitudes involved vary slowly with $r$. (i) Because $a^{+}_{s,\alpha}(r)$ varies slowly with $r$,

$$\left|\frac{d^2 a^{+}_{s,\alpha}}{dr^2}\right| \ll \left|k_\alpha \frac{da^{+}_{s,\alpha}}{dr}\right|, \tag{3.14}$$

and the second-derivative terms in Eqs. (3.6) may be dropped. (ii) Because the amplitude $\zeta_\alpha$ of the Coulomb functions varies very slowly with $r$,

$$\frac{d}{dr}\zeta_\alpha \ll k_\alpha \zeta_\alpha, \tag{3.15}$$

and $(d/dr)\zeta_\alpha$ may be neglected in Eq. (3.12), whence

$$\frac{1}{O_\alpha}\frac{dO_\alpha}{dr} = ik\zeta_\alpha. \tag{3.16}$$

With these approximations, the coupled equations (3.6) for the modulating amplitudes reduce to the first-order matrix equation

$$\frac{d}{dr}\vec{a}^{+}_s(r) = \mathfrak{M}(r)\vec{a}^{+}_s(r), \tag{3.17}$$

where the matrix $\mathfrak{M}$ is defined by

$$\mathfrak{M}_{\alpha\beta}(r) = -\frac{i}{2(k_\alpha k_\beta)^{1/2}} I_\alpha U^{c}_{\alpha\beta} O_\beta. \tag{3.18}$$

Equations (3.17) and (3.18) are identical to those derived by Alder, Morf, and Roesel[7] from the integral equivalent of the coupled equations (3.1); the differential derivation given here has the merit of exhibiting the two underlying approximations more explicitly.

Note that from Eq. (3.8) we can express the elements of $\mathfrak{M}$ as

$$\mathfrak{M}_{\alpha\beta} = -\frac{i}{2}\frac{U^c_{\alpha\beta}e^{-i(\phi_\alpha-\phi_\beta)}}{(k_\alpha\zeta_\alpha k_\beta\zeta_\beta)^{1/2}}\,. \tag{3.19}$$

Because from Eq. (3.9),

$$\phi_\alpha - \phi_\beta \sim (k_\alpha - k_\beta)r = \Delta k_{\alpha\beta} r\,, \tag{3.20}$$

it follows that the coupling matrix elements in Eq. (3.17) are slowly varying functions of $r$ modulated by oscillatory functions of wavelength $2\pi/(\Delta k_{\alpha\beta})$. Thus while the quadrature step length in the original coupled equations (3.1) is proportional to some average of $k_\alpha^{-1}$, that in the first-order amplitude equations is proportional to the minimum $(\Delta k_{\alpha\beta})^{-1}$. For heavy-ion reactions, $(\Delta k/k)^{-1}$ is typically of the order 10 or greater. The original set of second-order equations has thus been replaced by a first-order set that can be integrated with a much larger step length.

Yet another major simplification is possible. For the values of $r$ of interest here ($r > R_N \gg R_c'$), the deviations of $\vec{a}_s(r)$ from $\vec{a}_s(\infty)$ are small enough to permit solution of the amplitude equation (3.17) by the first term of a Born-Neumann series:

$$\vec{a}_s^{+(n)}(r) = \vec{a}_s^{+(n-1)}(r) + \int_\infty^r \mathfrak{M}(r')\vec{a}_s^{(n-1)}(r')dr'\,, \tag{3.21}$$

where the initial guess to be used is

$$a_{s,\alpha}^{+(0)}(r) = \sqrt{k_\alpha}\,\delta_{\alpha s}\,. \tag{3.22}$$

The first iteration of Eq. (3.21) gives the DWBA contribution to Coulomb excitation from $r$ to $\infty$:

$$a_{s,\alpha}^{+(1)}(r) = \sqrt{k_\alpha}\left(\delta_{\alpha s} - \int_r^\infty \mathfrak{M}_{\alpha s}(r')dr'\right). \tag{3.23}$$

### C. Recursion relations

Efficient techniques for the numerical evaluation of the integral appearing in Eq. (3.23) have been used for several years in the program Ptolemy[5] for the DWBA evaluation of inelastic scattering. Following the suggestion of Belling,[9] we can evaluate the integral as an asymptotic series in the lower limit $r$. The use of this asymptotic series makes it unnecessary to introduce the asymptotic radius $R_\infty$ into the calculation. Furthermore, simple recursion relations (in terms of the orbital angular momenta $l_\alpha$ and $l_s$) can be derived for the integrals. The use[5] of these recursion relations greatly accelerates the calculation. We derive the recursion relations in this subsection; similar relations have recently[10] been derived independently.

We consider integrals of the form

$$I_{l',l}^{(\lambda)} = \int_R^\infty dr\,\frac{1}{r^{\lambda+1}}\,Y_{l'}(\eta', k'r)X_l(\eta, kr)\,, \tag{3.24}$$

where $Y$ and $X$ designate Coulomb functions ($F$, $G$, $I$, or $O$). The lower limit of the integral may be zero if both $Y$ and $X$ are regular Coulomb functions. We will use the standard[11] Coulomb recursion relations:

$$l[(l+1)^2+\eta^2]^{1/2}X_{l+1} - (2l+1)\left(\eta + \frac{l(l+1)}{kr}\right)X_l + (l+1)[l^2+\eta^2]^{1/2}X_{l-1} = 0\,, \tag{3.25}$$

and

$$\frac{l}{k}\frac{d}{dr}X_l + \left(\eta + \frac{l^2}{kr}\right)X_l - [l^2+\eta^2]^{1/2}X_{l-1} = 0\,. \tag{3.26}$$

Equation (3.26) may be used to eliminate $X_{l-1}$ from Eq. (3.25):

$$X_{l+1} = \frac{l+1}{[(l+1)^2+\eta^2]^{1/2}}\left(\frac{\eta}{l+1} + \frac{l+1}{kr} - \frac{1}{k}\frac{d}{dr}\right)X_l\,. \tag{3.27}$$

This may be substituted in Eq. (3.24) for $I_{l',l+1}^{(\lambda)}$ to yield

$$I_{l',l+1}^{(\lambda)} = \frac{l+1}{[(l+1)^2+\eta^2]^{1/2}}\left(\frac{\eta}{l+1}I_{l',l}^{(\lambda)} + \frac{l+1}{k}I_{l',l}^{(\lambda+1)} - \frac{1}{k}\int_R^\infty dr\,\frac{1}{r^{\lambda+1}}Y_{l'}\frac{d}{dr}X_l\right). \tag{3.28}$$

The derivative in the last integral in Eq. (3.28) may be moved to $Y_{l'}$ by integration by parts. Then using Eq. (3.26) to eliminate $(d/dr)Y_{l'}$, we obtain

$$\int_R^\infty dr\,\frac{1}{r^{\lambda+1}}\,Y_{l'}\frac{d}{dr}X_l = -J_{l',l}^{(\lambda)} + \frac{k'\eta'}{l'}I_{l',l}^{(\lambda)} - \frac{k'(l'^2+\eta'^2)^{1/2}}{l'}I_{l'-1,l}^{(\lambda)} + (\lambda+l'+1)I_{l',l}^{(\lambda+1)}\,, \tag{3.29}$$

where

$$J_{l',l}^{(\lambda)} = \frac{1}{R^{\lambda+1}}Y_{l'}(\eta', k'R)X_l(\eta, kR)\,. \tag{3.30}$$

If we substitute Eq. (3.29) in Eq. (3.28) and use Eq. (3.25) to express $I_{l',l}^{(\lambda+1)}$ in terms of $I_{l',l-1}^{(\lambda)}$, $I_{l',l}^{(\lambda)}$, and $I_{l',l+1}^{(\lambda)}$, we obtain an expression for $I_{l',l+1}^{(\lambda)}$ in terms of $I_{l'-1,l}^{(\lambda)}$, $I_{l',l-1}^{(\lambda)}$, $I_{l',l}^{(\lambda)}$, and $I_{l',l+1}^{(\lambda)}$. This may be solved for $I_{l',l+1}^{(\lambda)}$ to yield the recursion relation:

$$I^{(\lambda)}_{l',l+1}=\frac{l+1}{k(l+l'+\lambda+1)[(l+1)^2+\eta^2]^{1/2}}\left[(2l+1)\left(\eta k\frac{l'+\lambda}{l(l+1)}-\eta' k'\frac{1}{l'}\right)I^{(\lambda)}_{l',l}+k'\frac{2l+1}{l'}(l'^2+\eta'^2)^{1/2}I^{(\lambda)}_{l'-1,l}\right.$$
$$\left.+k\frac{l-l'-\lambda}{l}(l^2+\eta^2)^{1/2}I^{(\lambda)}_{l',l-1}+(2l+1)J^{(\lambda)}_{l',l}\right]. \qquad (3.31)$$

By symmetry we can interchange $l$ with $l'$, $\eta$ with $\eta'$, and $k$ with $k'$ in Eq. (3.31) to yield a recursion relation for $I^{(\lambda)}_{l'+1,l}$ in terms of the same quantities that appear in Eq. (3.31).

Consider even $\lambda$. If we have $I^{(\lambda)}_{L-\delta,L-l+\delta}$ for $\delta=-\lambda/2+1,\ -\lambda/2+2,\ldots,\lambda/2$ and $I^{(\lambda)}_{L-\delta,L+\delta}$ for $\delta=-\lambda/2,\ldots,\lambda/2$, then the two recursion relations may be used to generate first $I^{(\lambda)}_{L+1-\delta,L+\delta}$ for $\delta=-\lambda/2+1,\ldots,\lambda/2$ and then $I^{(\lambda)}_{L+1-\delta,L+1+\delta}$ for $\delta=-\lambda/2,\ldots,\lambda/2$. These may then be used to go on to $L+2$, and so forth. A similar scheme may be used for odd $\lambda$. Thus we need only $2\lambda+1$ initial values of $I^{(\lambda)}_{l',l}$ to generate all of the required $I^{(\lambda)}_{l',l}$. These initial values may be computed by numerical quadrature of Eq. (3.24) or, as previously mentioned, from an asymptotic expansion in $R$.

We have tested the stability of these recursion relations for many cases. Unless $R=0$, the upward recursion relations are only slightly unstable for all combinations of Coulomb functions; one or two decimal places may be lost in 1000 iterations. Downward recursion relations analogous to Eq. (3.31) may be developed for $\int_0^\infty dr F_l F_{l'}/r^{\lambda+1}$; we shall not give the results here.

### D. Asymptotic expansions for coupled-channel Coulomb functions

Asymptotic series expansions in powers of $1/r$ have been given[12] for the coupled-channels Coulomb functions $\mathcal{O}_{s,\alpha}$ and $\mathcal{I}_{s,\alpha}$. In the adiabatic limit, the coupled-channels asymptotic series are straightforward matrix generalizations of the single-channel series. The coefficients are given by three-term recursion formulas. Ten-figure accuracy can still be achieved from these series at distances less than twice the turning-point radius. Inclusion of the effects of nonadiabaticity significantly complicates matters. The three-term recursion relations for the expansion coefficients are replaced by four-term recursion relations whose leading terms are proportional to the energy differences $\Delta E_{\alpha\beta}$ between channels. Such recursion formulas are numerically ill-conditioned; for extensive use it would probably be necessary to develop some form of perturbation expansion in $\Delta E$ based on the adiabatic limit as unperturbed solution. The numerical effort involved for all necessary $J$ values is in any case considerably greater than that involved in evaluating the Alder-Pauli amplitudes by the techniques described above. This comparison depends on the accuracy of the first-order reduction of the equations for the modulating amplitudes and of the Born solution of the first-order equations. In case of failure of the Born solution of the reduced first-order equations, it would be necessary to reassess the merits of direct use of the asymptotic expansions for the coupled-channels Coulomb functions.

## IV. NUMERICAL STUDIES OF THE MODULATING FUNCTIONS

### A. Accuracy of approximations for the modulating functions

We now discuss the accuracy of the three approximations introduced in the previous section for the modulating functions: (1) Neglect of the second-derivative terms in the Eq. (3.6), resulting in a set of first-order equations for the amplitudes $\vec{a}_s$; (2) neglect of the derivatives $(d/dr)\zeta_\alpha$ of the amplitudes of the single-channel Coulomb functions in computing the coupling terms in the first-order equations; and (3) use of the Born approximation to integrate the first-order equations inwards from $r=\infty$ to distances $r$ of the order of the outer limit $R_N$ of the "nuclear" interior region.

The following coupled channels are considered

Channels

| | Elastic | Excited | $E_{\rm Lab}$ | $\eta$ |
|---|---|---|---|---|
| (a) | $^{18}O+^{184}W$ | $^{18}O+^{184}W(2^+,\ 0.111\ MeV)$ | 90 | 41.7 |
| (b) | $^{132}Xe+^{208}Pb$ | $^{132}Xe(2^+,\ 0.668\ MeV)+^{208}Pb$ | 800 | 283.2 |
| (c) | $^{16}O+^{44}Ca$ | $^{16}O+^{44}Ca(2^+,\ 1.156\ MeV)$ | 60 | 13.0 |

where the projectile is listed first and the values of $\eta$ refer to the elastic channel. Optical-model and deformation parameters for the calculations to be reported are given in the appropriate figure captions. In all of the calculations reported in this section, reorientation effects (couplings within the excited channel) have been ignored; we have verified that their inclusion does not affect our conclusions.

To simplify notation for the modulating amplitudes and $S$-matrix elements, we use the following labeling for the four reaction channels for given angular momentum $J$ ($>2$) in the reactions involving $2^+$ excitation:

$$\begin{aligned} &\alpha=1;\ 0^+,\ l=J \\ &\alpha=2;\ 2^+,\ l=J-2 \\ &\alpha=3;\ 2^+,\ l=J \\ &\alpha=4;\ 2^+,\ l=J+2. \end{aligned} \tag{4.1}$$

*Reaction (a)*, $^{18}O+^{184}W$ at $E_{Lab}=90$ MeV. Figure 1 shows the modulus of the amplitude $a^+_{1,3}(J=50)$ in the critical partial wave; $a^+_{1,3}$ is the amplitude in channel 3 of the outgoing-wave solution of Eqs. (3.6) that tends asymptotically to an outgoing wave in channel 1. For comparative purposes the amplitudes have been divided by $\sqrt{k_3}$. In this reaction, the main source of error is neglect of the second-derivative terms in Eqs. (3.6); the relative error in $a_{1,3}$ is around 2% all the way in to 15 fm (the turning point for $l=50$ is at 13.5 fm). The additional approximations—neglect of $(d/dr)\zeta$ and Born approximation solution of the first-order equations—introduce negligible errors less than 0.1% for $r>15$ fm. Figure 1 also shows the modulus of the error in the Born amplitude $|a_{1,3}(\text{Born})-a_{1,3}(\text{exact})|$; this error is of the order of 1% of the magnitude of the amplitude $a_{1,1}$ [the one that according to Eqs. (3.4) approaches $\sqrt{k_1}$ as $r\to\infty$].

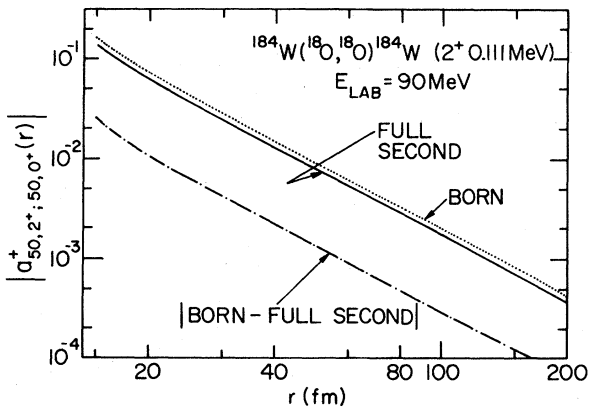


FIG. 1 A comparison of the modulus of the amplitude $a^+_{1,3}(J=50)$ calculated using the full second-order equation (3.6) and the Born approximation (3.23). The modulus of the error in the Born amplitude $|a_{1,3}(\text{Born})-a_{1,3}(\text{exact})|$ is also shown. The amplitudes have been divided by $\sqrt{k_3}$. The Coulomb coupling had $\beta^C_2=0.234$.

*Reactions (b)*, $^{132}Xe+^{208}Pb$ at $E_{Lab}=800$ MeV. This reaction may be treated semiclassically with high accuracy. The first-order reduction of the amplitude equations introduces negligible errors; for $J=100$, neglect of second-derivative terms in Eq. (3.6) results in a relative error in $a_{1,3}$ ($J=100$) of 0.16% at $r=25$ fm. The Born approximation is the dominant source of error, yielding a 10% error in $a_{1,3}$ at 25 fm, 1% at 40 fm.

*Reaction (c)*, $^{16}O+^{44}Ca$ at $E_{Lab}=60$ MeV. This reaction does not lend itself to a semiclassical treatment, and the neglect of the second-derivative term introduces the largest error—2% in $a_{1,3}(J=4)$ at 20 fm. Neglect of $(d/dr)\zeta$ introduces an additional relative error of 0.06%, and the Born approximation 0.2% at 20 fm. However, the departures of the $a$'s from their asymptotic values are quite small $[|a(r=20)-a(r=\infty)|\sim 0.02]$ so that these percentage errors represent negligible absolute errors.

These results illustrate our conclusions, drawn from studies of a wide variety of reactions. For very strong Coulomb fields (large $\eta$), errors due to the first-order reduction of the amplitude equations are small, the amplitudes themselves deviate strongly from their asymptotic values [Eqs. (3.4)] and the dominant source of error is the Born approximation. For reactions with small values of $\eta$, the main source of error is the neglect of second derivatives in Eqs. (3.6); the modulating amplitudes for $r>R_N$ do not deviate strongly from their asymptotic values [Eqs. (3.4)], and the errors due to the Born approximation are negligible. In such cases, because the deviations from the asymptotic values are small, the moderately large relative errors introduced by the neglect of the second-derivative terms result in very small errors in $S$-matrix elements and cross sections. In general, the Born approximation (3.23) to the solution of the approximate first-order equation (3.17) permits calculation of the modulating amplitudes $a^\pm_s(r)$ in Eqs. (3.3) inwards from $r=\infty$ to typical nuclear matching radii, $R_N\sim 20$ to 30 fm, with errors of a few percent.

### B. Sensitivity of $S$-matrix elements and cross sections to errors in the modulating functions

It remains to be seen whether "few percent" errors in the modulating amplitudes lead to significant errors in computed $S$-matrix elements and cross sections. The modulating amplitudes are used through Eqs. (3.3) to construct a com-

plete set of outgoing solutions $\vec{\mathcal{O}}_s$ and an incoming solution $\vec{\mathcal{I}}_{\alpha_0}$ of the coupled equations (3.1) for Coulomb excitation. These coupled Coulomb functions are then matched at the joining radius $R_N$ to solutions of the original coupled Eqs. (2.6) in the interior region. The techniques used to produce interior solutions will be discussed in the second paper of this series.

Figure 2 shows the $S$-matrix elements $S_{11}$ (elastic) and $S_{31}$ (inelastic), in the $J=50$ partial wave for reaction (a), obtained from matching procedures of the sort described using $a$'s computed by the Born approximation. The magnitudes of the $S$-matrix elements obtained by matching at a variety of values $R_N$ from 75 to around 20 fm are compared with exact values. It is clear that the modified matching procedure yields $S$-matrix elements of satisfactory accuracy. Figure 2 also shows the $S$-matrix elements obtained by matching at $R_N$ to single-channel Coulomb functions (the traditional matching procedure). Accurate results are not obtained until $R_N > 75$ fm, with large discrepancies at values of $R_N$ of practical interest ($\lesssim 30$ fm). The differential cross sections for reaction (a) obtained using Born $a$'s at various matching radii are compared in Fig. 3 with each other and with what is obtained by matching to single-channel Coulomb functions. The Born $a$'s

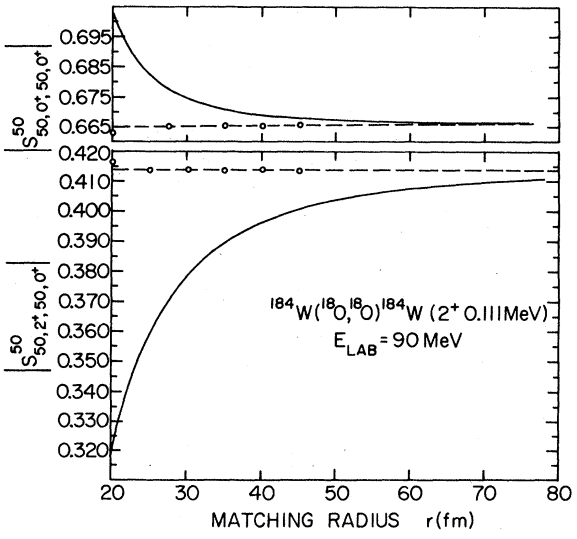


FIG. 2. The solid lines represent the modulus of the elastic and one inelastic $S$-matrix elements obtained by matching to single channel Coulomb functions at various radii $r$. The dashed lines represent the converged results, and the open circles show the values obtained using the Born approximation to the amplitude function with the matching equation (3.5). All calculations were performed using complex Woods-Saxon potentials of equal geometry with the parameters $V=40$, $W=25$, $r_0=1.29$, $a=0.508$, $r_{c0}=1.2$, $\beta_2^N=0.145$, and $\beta_2^C=0.234$.

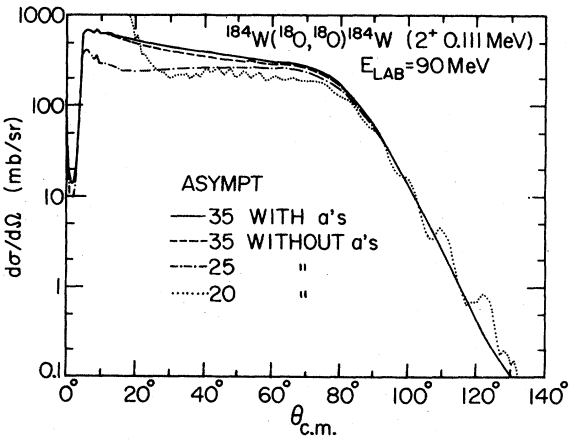


FIG. 3. A comparison of the inelastic cross sections calculated using $S$-matrix elements derived from the matching equations (2.9) and (3.5) at various matching radii $r$. The results using Eq. (3.5) are indistinguishable for matching radii $\geq 20$ fm. The cross sections for $\theta_{c.m.} < 15°$ are inaccurate because of the orbital angular momentum truncation ($l,l' \leq 1000$). The potential parameters are the same as for Fig. 2.

yield the cross section accurately for matching radii $R_N$ as small as 20 fm; the errors in the cross sections obtained by matching to single-channel Coulomb functions are large.

The main conclusions, confirmed by the results of many other calculations, are (i) Coulomb-coupling effects in the intermediate region ($R_N < r < R_\infty$) have a large influence on $S$-matrix elements and cross sections; and (ii) these effects are accounted for accurately and efficiently on the basis of the Alder-Pauli factorization (3.3) of the solutions of the coupled equations for Coulomb excitation, with the first Born approximation for the modulating amplitudes.

## V. QUALITATIVE ASPECTS OF THE ALDER-PAULI PROCEDURE

The procedure established above for dealing with intermediate-range effects of Coulomb excitation involves matching interior solutions of the coupled equations to combinations of incoming and outgoing solutions $\vec{\mathcal{I}}_s$, $\vec{\mathcal{O}}_s$ of the coupled equations for Coulomb excitation. The matching radii $R_N$ can then be taken to be of "nuclear" size (20 to 30 fm). The coupled-channels Coulomb functions take over the role of ordinary Coulomb functions $I_\alpha, O_\alpha$ in the matching procedures of conventional optical-model and coupled-channels calculations. For this modified matching procedure to be computationally feasible it is essential that the coupled-channels Coulomb functions be computed efficiently. Direct integration of the original coupled equations from $R_\infty$ to $R_N$ is out

of the question; indeed it was the extreme inefficiency of such integrations across the intermediate region of $r$ space that triggered the search for modified procedures. The Alder-Pauli factorization (3.3) is the basis of our technique for construction of the coupled-channels Coulomb functions. Its great efficiency depends on the validity of three approximations for the modulating functions.

(1) Neglect of second derivatives in the coupled equations (3.6) for the modulating functions. This first-order reduction greatly enhances the value of the Alder-Pauli transformation. Direct numerical integration of the second-order equations (3.6) is a difficult numerical task, in spite of the fact that the modulating amplitudes vary slowly with $r$, because second-order equations that are approximately of first order are numerically awkward.

(2) Neglect of the derivatives $(d/dr)\zeta_\alpha$ of the amplitudes of the single-channel Coulomb functions. It is this approximation that permits the Born solution (3.23) to be written in terms of the DWBA matrix elements for Coulomb excitation. These integrals satisfy simple recursion formulas that enormously reduce the numerical labor involved in evaluating the coupled-channel Coulomb functions. Errors due to neglect of $(d/dr)\zeta_\alpha$ are always negligible relative to those involved in the first-order reduction of Eqs. (3.6).

(3) Use of the first Born approximation (3.23) to solve the first-order equations for $a_s$. The accuracy of this approximation depends on the fact that for distances of interest ($r \gtrsim 20$ fm) in a large class of reactions, the modulating amplitudes deviate in magnitude by $0.2\sqrt{k_\alpha}$ or less from their asymptotic values (3.4). When the Born approximation is reasonable, the errors involved should be of the order of the second-order correction and hence proportional to $|a_{s,\alpha}-\sqrt{k_\alpha}\delta_{s\alpha}|^2$. Thus the magnitudes of the Born amplitudes can be used as an error indicator; if any of the quantities $|a_{s,\alpha}|^2/k_\alpha$ for $\alpha \neq s$ at $R_N$ exceed some desired accuracy, consideration should be given to increasing the matching radius. (Note that in the Born approximation $a_{s,s}=\sqrt{k_s}$ .)

By using these techniques, one can compute heavy-ion coupled-channels scattering amplitudes involving strong Coulomb excitation in much the same time as if there were no long-range component to the Coulomb coupling.

## ACKNOWLEDGMENTS

We thank Dr. Fritz Coester for helpful discussions and for a critical reading of the manuscript. This work was supported by the U. S. Dept. of Energy.

[1]K. Alder and A. Winther, K. Dan. Vidensk. Selsk., Mat. Fys. Medd. 32, No. 8 (1960).
[2]K. Alder and H. C. Pauli, Nucl. Phys. 128, 1931 (1969).
[3]L. Schlessinger and G. L. Payne, Phys. Rev. A 10, 1559 (1974).
[4]J. Raynal in *Computing as a Language of Physics*, (IAEA, Vienna, 1972), p. 281.
[5]M. H. Macfarlane and S. C. Pieper, Argonne Nat. Lab. Report No. ANL-76-11, Rev. 1, 1978 (unpublished).
[6]G. R. Satchler in *Lectures in Theoretical Physics*, Vol. VIII-C, edited by P. D. Kunz, D. A. Lind, and W. E. Britten (Univ. of Colorado Press, Boulder, 1966), p. 73.
[7]K. Alder, F. Roesel, and R. Morf, Nucl. Phys. A284, 145 (1977).
[8]M. J. Seaton and G. Peach, Proc. Phys. Soc. London 79, 1296 (1962).
[9]J. A. Belling, J. Phys. B 1, 136 (1968).
[10]L. E. Wright, Phys. Rev. C 20, 393 (1979).
[11]M. Abramowitz in *Handbook of Mathematical Functions*, edited by M. Abramowitz and I. A. Stegun (U.S. Government Printing Office, Washington, 1964), p. 537.
[12]F. Rösel, K. Alder, R. Morf, and J. X. Saladin, J. Phys. G 3, 613 (1977).